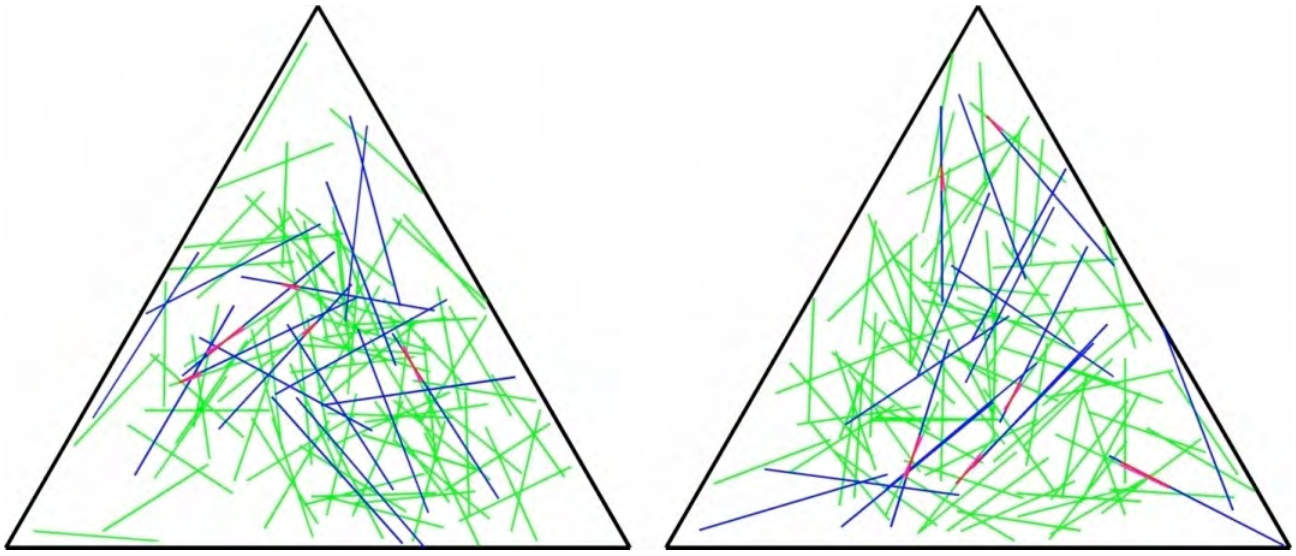

Fig. S1. Two examples of computationally generated random distributions of MTs (green) and F-actin bundles (blue). Overlap regions are colored red. For the realization in the left triangle, $L_{MT\text{-}AB}$ / L_{MT}=0.013 and $L_{AB\text{-}MT}$/ L_{AB}=0.041; for the realization in the right triangle, $L_{MT\text{-}AB}$ / L_{MT}=0.020 and $L_{AB\text{-}MT}$/ L_{AB}=0.063.

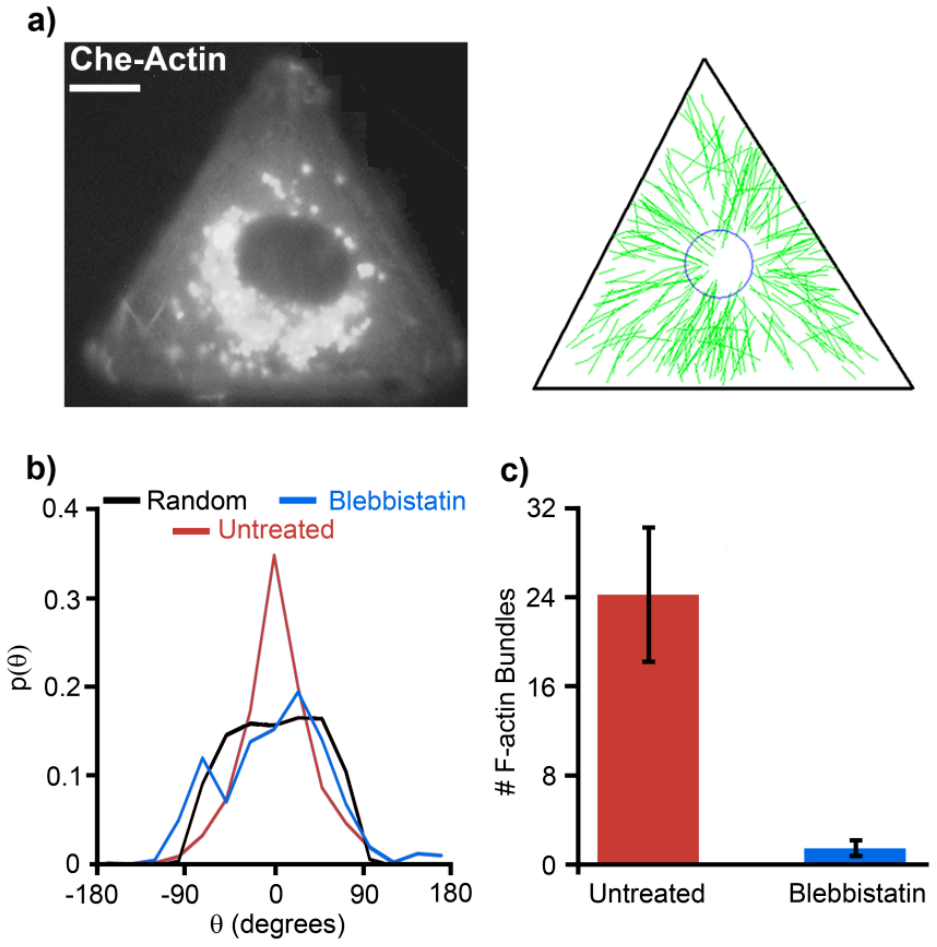

Fig. S2. The effect of blebbistatin on actin bundle depletion and directed/guided MT growth towards FAs/vertices. Rat2 cells on triangular, fibronectin-coated islands were either untreated (see Fig. 4 in the main text) or treated with **(a)** specific inhibitor for non-muscle myosin II, blebbistatin (25 μM) to deplete interior bundles. (Left panel in a) Cherry-Actin images showing a typical cell with depleted F-actin bundles and (right panel in a) corresponding reconstructed MT growth trajectories (green tracks); triangle shows cell boundary. Scale bar is 10 μm. **(b)** Probability distributions of the MT growth directions; red, untreated; blue, Blebbistatin; black, random/unguided. Data for Blebbistatin treatment is based on 280 trajectories from two cells. (**c**) Quantification of the extent of F-actin bundle depletion. Blebbistatin depletes interior F-actin bundles which leads to "random/unguided" MT growth directions.

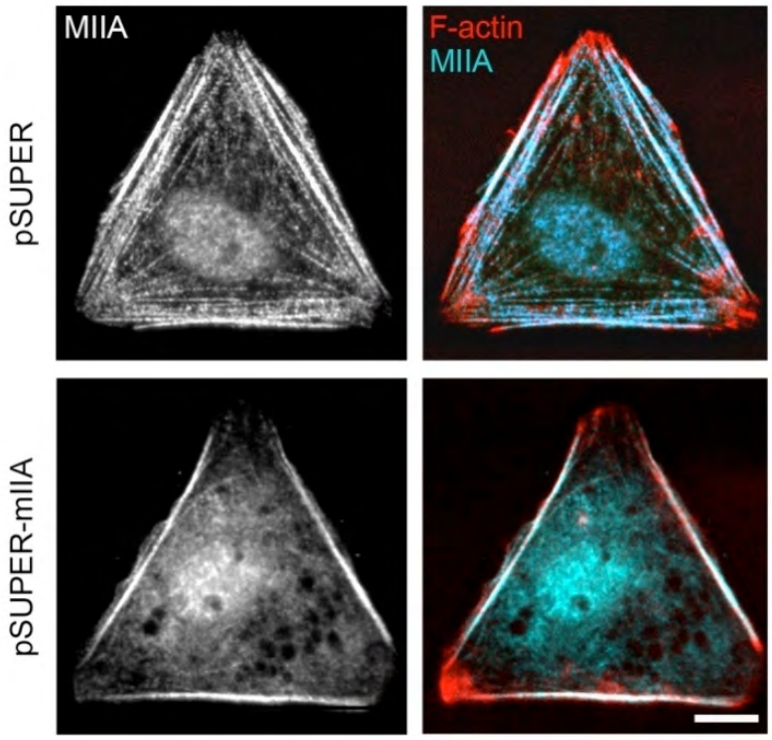

Fig. S3. Depletion of F-actin bundles in triangular cells by knockdown of myosin IIA. Visualization of F-actin bundles (red in right panels) by fluorescent phalloidin staining and myosin IIA (MIIA, cyan in right panel) by immunostaining with antibody to mIIA in control cells (pSUPER) and in cells with depleted mIIA (pSUPER-mIIA). Note that MIIA-depleted cells (bottom) apart from edge bundles display no internal F-actin bundles, while control cells (top) display numerous F-actin bundles marked by MIIA. Quantification of knockdown effect is shown in Fig. 6E in the main text. Scale bar is 10 μm.

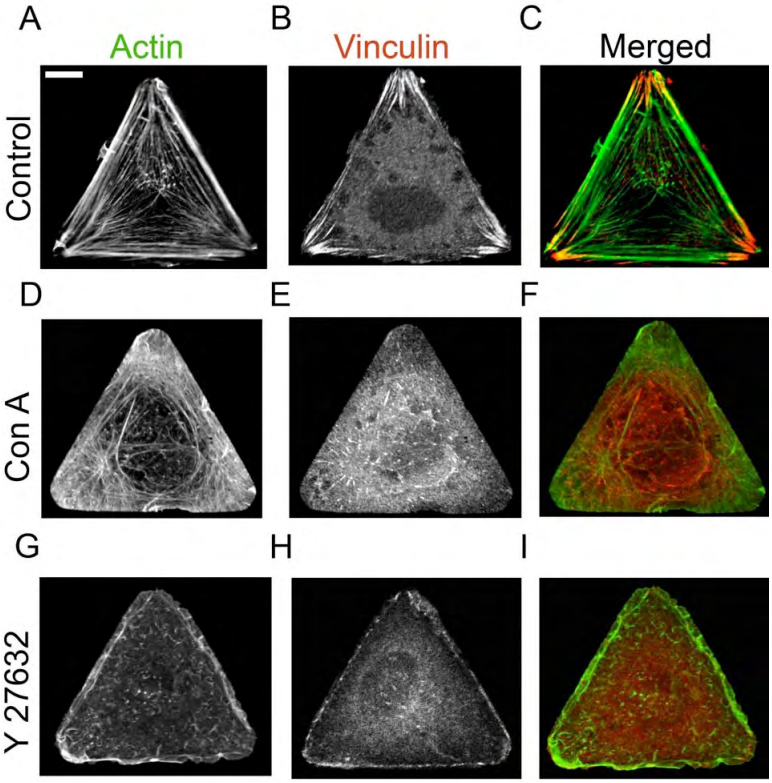

Fig. S4. Distribution of F-actin (Actin) and focal adhesions (Vinculin). Control=untreated cells on fibronectin; ConA=untreated cells on Concanavalin A substrate; Y27632=cells on fibronectin substrate treated with Y27632. Scale bar is=10 μm and is the same for all images.

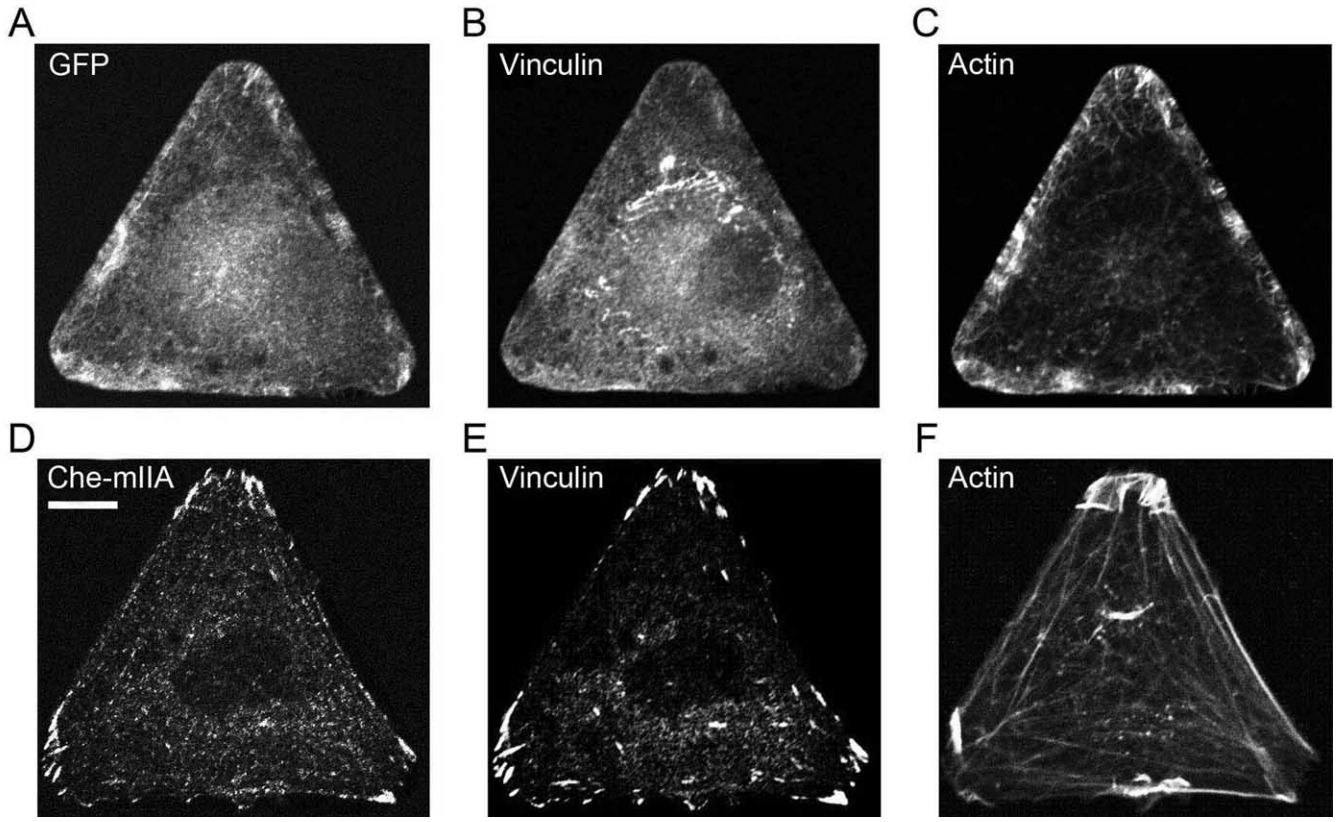

Fig. S5. Focal adhesion and F-actin distribution in cells with depleted MIIA and rescued knockdown cells. Focal adhesion/F-actin distribution for experiments corresponding to Fig. 6. Cells were co-transfected with GFP-EB3 to mark transfected cells and pSUPER-MIIA to deplete MIIA (knockdown, panels a-c) or with pSUPER-MIIA and RNAi resistant Che-mIIA (rescue, panels D-F). F-actin is visualized by staining with fluorescent phalloidin, focal adhesions are visualized by immunostaining for Vinculin. GFP indicates transfected cells for a-c and Che-mIIA indicates transfected cells for D-F. Scale bar is 10 μm and corresponds to all images.

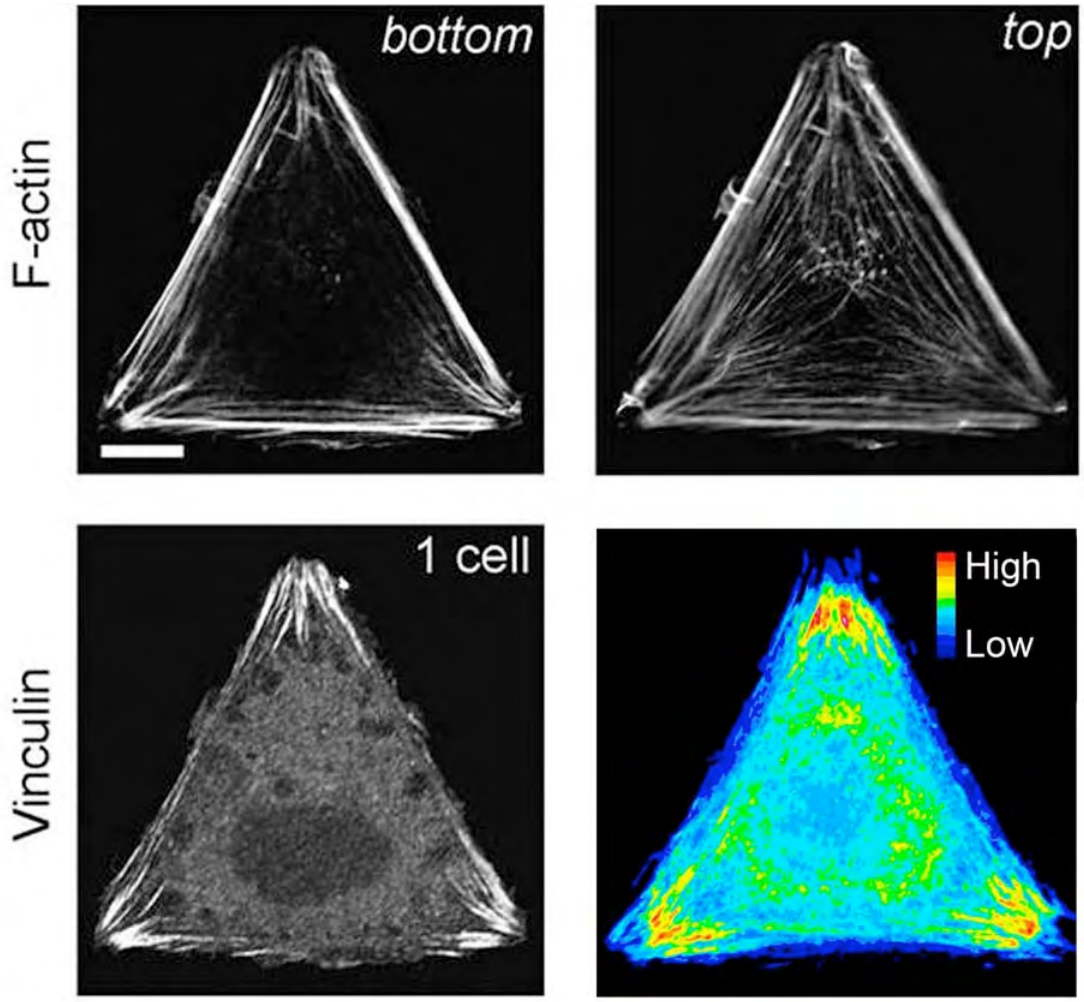

Fig. S6. Typical distribution of F-actin bundles and focal adhesions in triangular cells. Rat2 cells were cultured on triangular fibronectin micropatterns. F-actin and focal adhesions were visualized by staining with fluorescent phalloidin or immunostaining with vinculin antibody, respectively. Two representative planes – bottom and top – from z-stack obtained by confocal microscopy are shown for F-actin. The plane closer to the substratum (labeled "bottom") features strong edge bundles and no internal bundles (or occasionally some randomly organized bundles). The bundles emanating from the corners into cell interior originate at the bottom plane (as small "stumps") and extend into the upper planes indicating that these bundles are slanted upwards. The entire organization is visualized more precisely in these confocal images versus live wide field images shown in Figures 4 and 5 in the main text. For vinculin, one representative image (1 cell) and population average of 25 such images (pseudocolored heatmap) is shown. FAs localize predominantly to the vertices. Scale bar is 10 μm and is the same for all images.

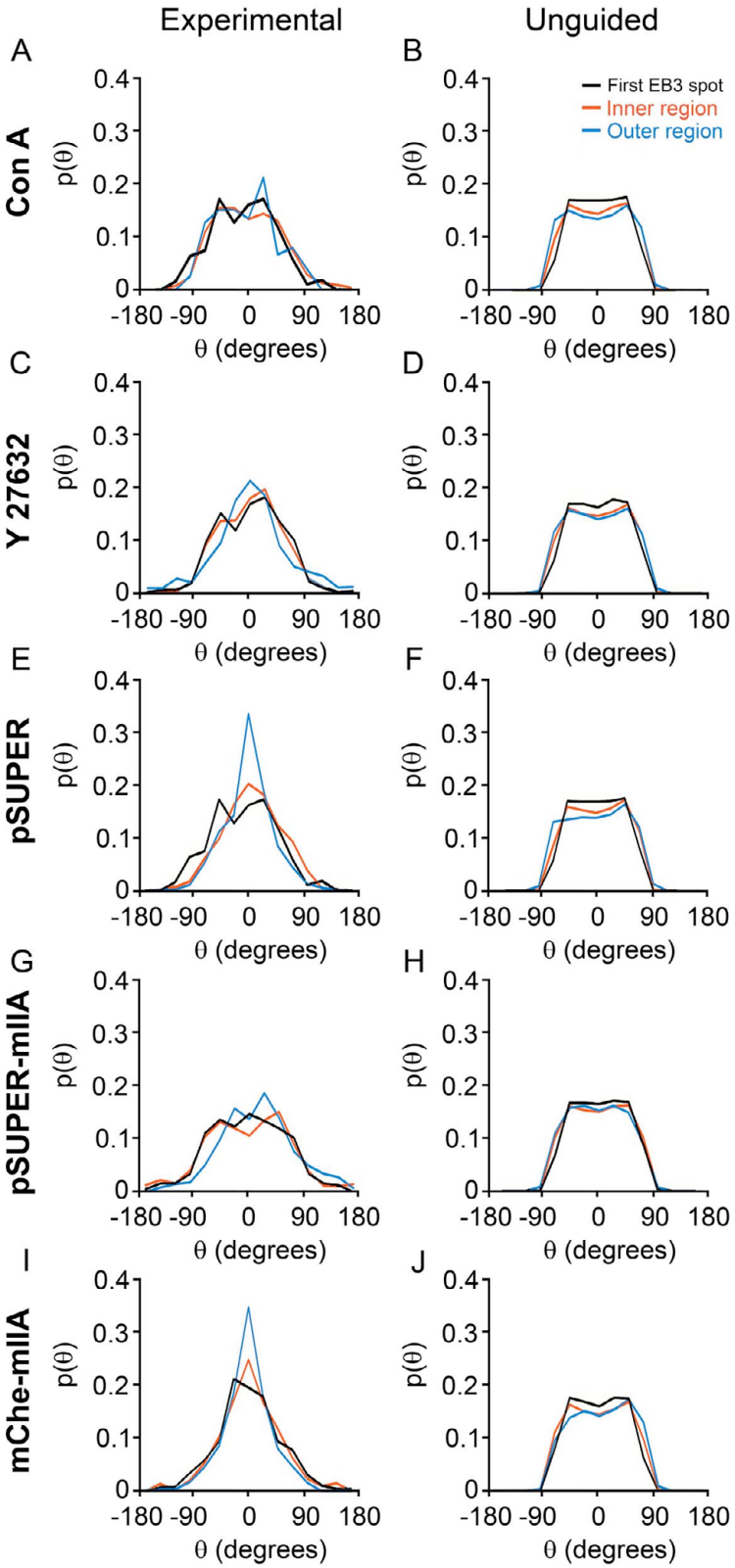

Fig. S7. Regional analysis of the directions of MT growth trajectories upon F-actin bundle depletion. MT trajectories were tracked in Rat2 cells cultured on triangular fibronectin (C-J) or Con A micropatterns (A,B). (A, C, E, G, I) show MT trajectories obtained from experiments (corresponding to Figs 2 and 5); (B, D, F, H, J) show corresponding 'unguided' trajectories generated computationally. MT trajectories were analyzed as illustrated in Fig. 3. Note that outer region represents annular region inscribed within the triangle. For cells on Con A substrate (A,B), MT growth directions are random/unguided for all three regions (compare to analysis for cells on fibronectin shown in Fig. 3). For treatment with Y27632 (C,D) and transfection with pSUPER-MIIA (G,H) also all three regions show random/unguided MT trajectories. In contrast, cells transfected with control pSUPER vector (E,F) or with pSUPER + mChe-mIIA (mChe-mIIA, rescue; I, J) show guided MT trajectories in two annular shells (inner and outer region) similar to untreated control cells (shown in Fig. 3) while MT nucleation (First EB3 spot) is without preference in direction.

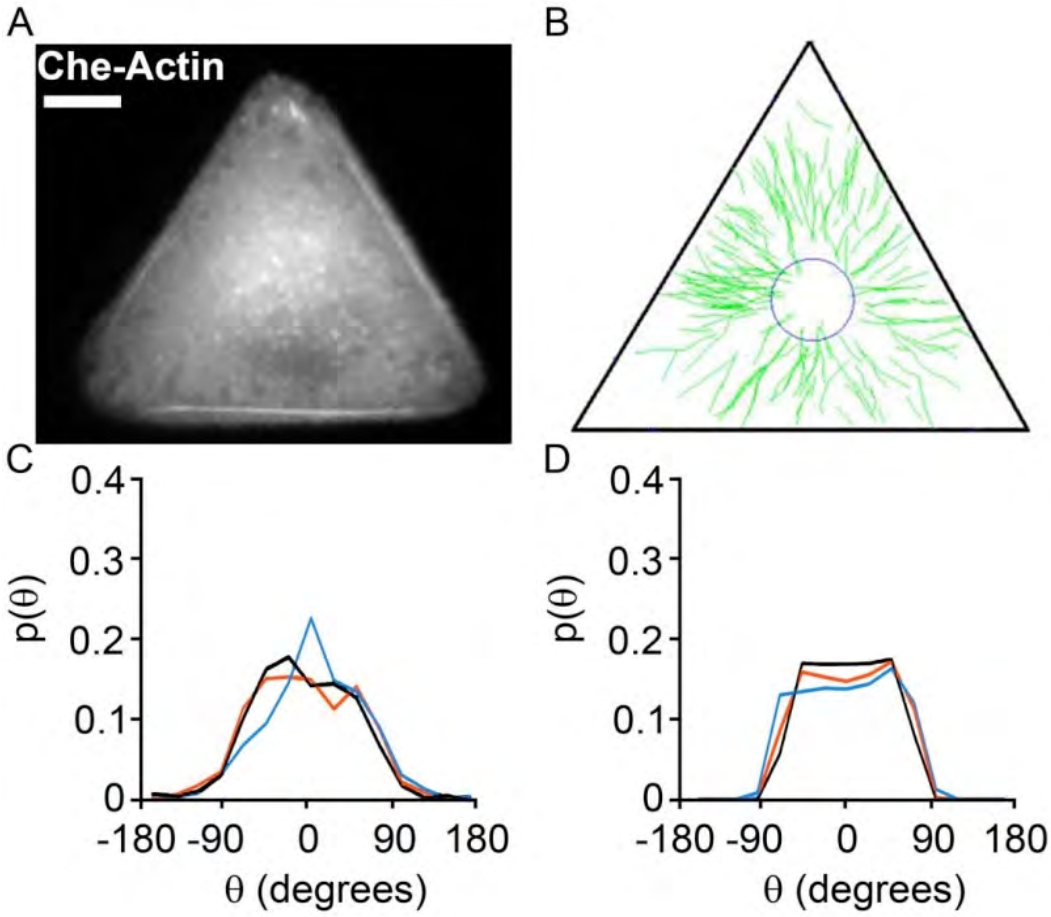

Fig. S8. The effect of depletion of myosin IIB on MT guidance. (A) Che-Actin image of cells transfected with pSUPER-MIIB showing that most large F-actin bundles are depleted. (B) MT growth trajectories in cells without mIIB. Probability distributions of MT growth directions in (C) cells without mIIB (experimental data) and (D) corresponding trajectories for random/unguided scenario (computationally generated data). Data analyzes as shown in Fig. 3. Scale bar is 10 μm.

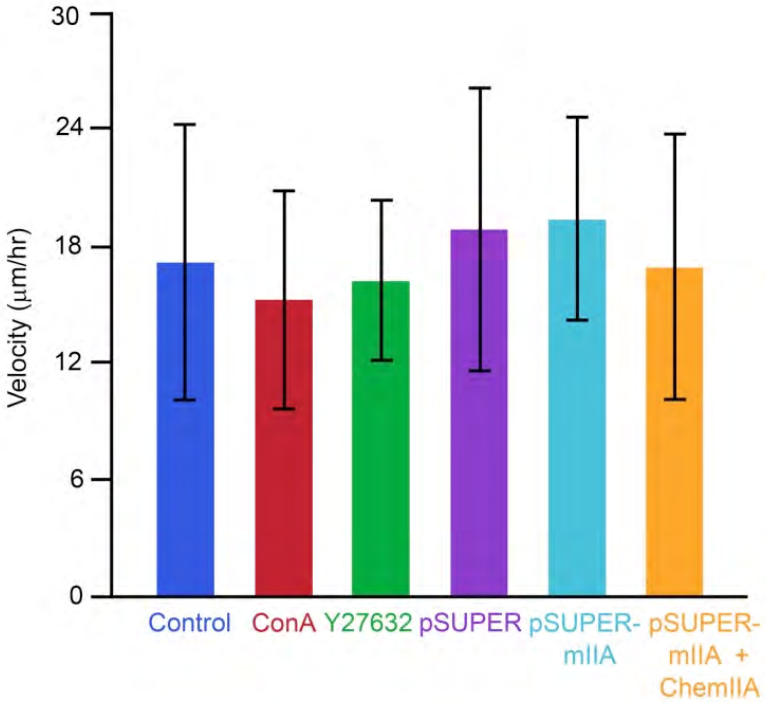

Fig. S9. The MT growth rates in triangular cells subjected to various treatments. Data shown is mean ± s.d., there are no statistical differences between the groups. Student's *t*-test was performed to compare all treatment groups to the control cells. The test showed that there was no statistical difference between the groups.

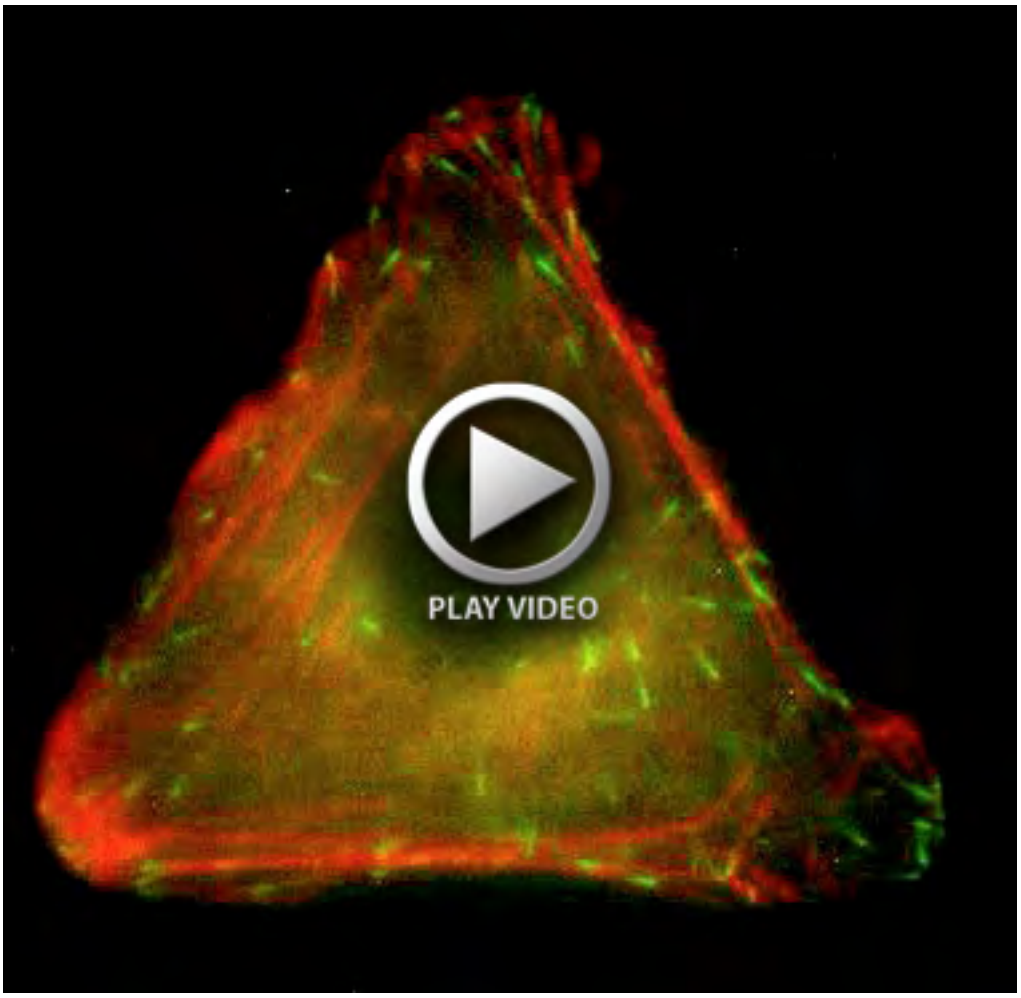

Movie 1. Microtubule growth trajectories and F-actin bundles in triangular cells. Rat2 cells were co-transfected with EB3-GFP and mCherry-actin and constrained onto triangular micropatterns (Pattern Area ~ 1256 μm^2). Microtubule growth and F-actin bundles were visualized using time-lapse dual-fluorescence digital microscopy. Total time of the movie is 7 minutes.

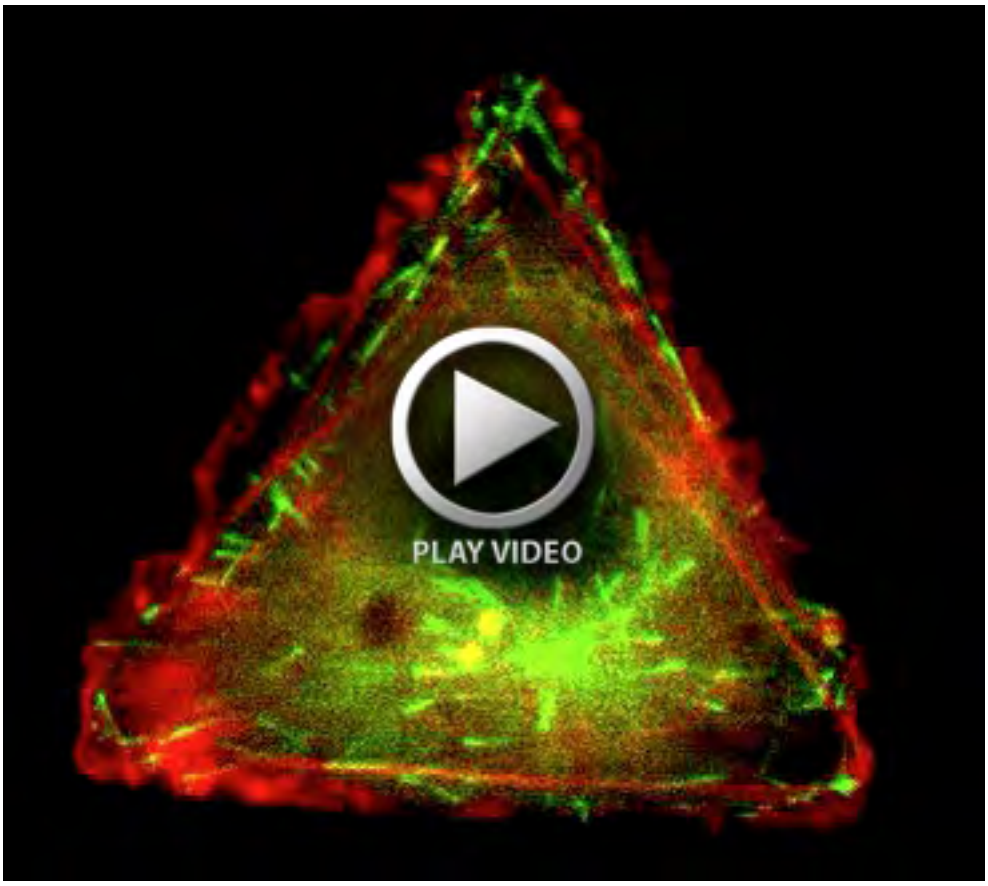

Movie 2. Microtubule growth trajectories and F-actin bundles in triangular cells. This is another example showing microtubule growth and F-actin bundles in a micropatterned cell. Total time of the movie is 7 minutes.

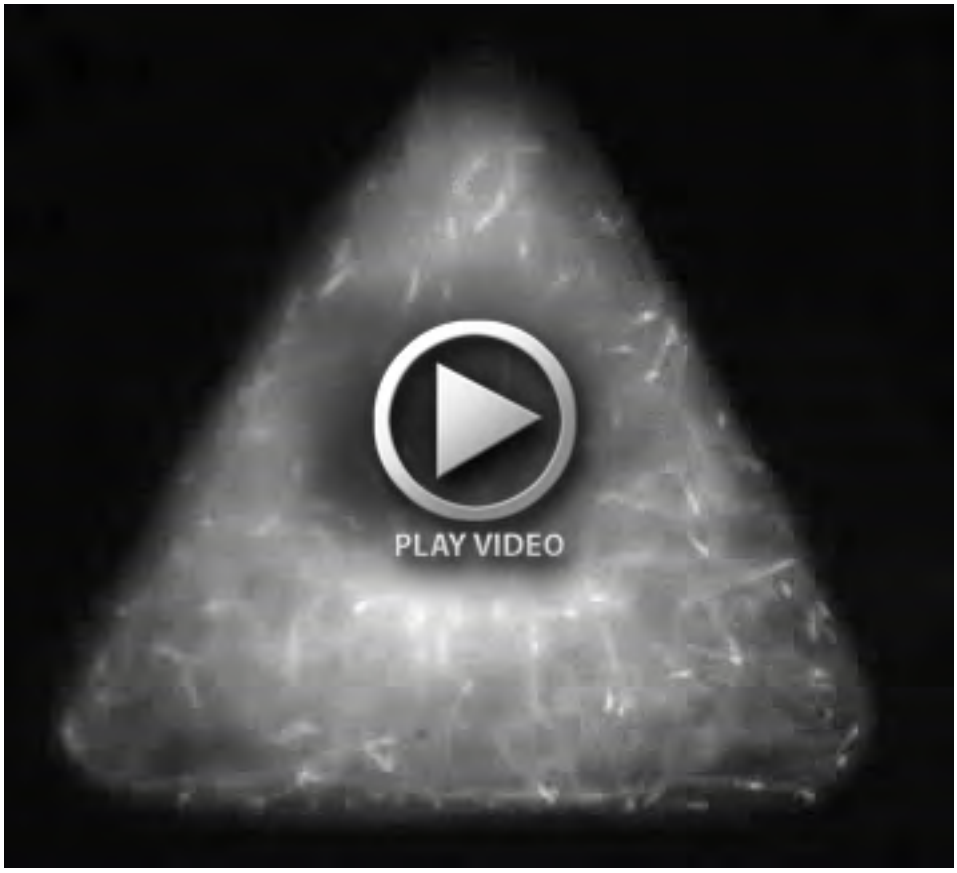

Movie 3. Microtubule growth trajectories and F-actin bundles in cells treated with Rho Kinase (ROCK) inhibitor Y27632. Cells were co-transfected with EB3-GFP and mCherry-Actin. The cells were then allowed to spread onto triangular micropatterns and then treated with 60 μM Y27632. Total time of the movie is 7 minutes.